AGU PUBLICATIONS

Geophysical Research Letters

RESEARCH LETTER
10.1002/2015GL066396

Key Points:
- Ratio between seasonal variability of precipitation and streamflow decomposed under Budyko framework
- Control of climate aridity, seasonality in precip, and its coupling with ET on catchment responses
- Vegetation plays an important role when the climate seasonality is weak

Supporting Information:
- Supporting Information S1

Correspondence to:
H.-Y. Li,
hongyi.li@pnnl.gov

Citation:
Ye, S., H.-Y. Li, S. Li, L. R. Leung, Y. Demissie, Q. Ran, and G. Blöschl (2015), Vegetation regulation on streamflow intra-annual variability through adaption to climate variations, *Geophys. Res. Lett.*, *42*, 10,307–10,315, doi:10.1002/2015GL066396.

Received 29 SEP 2015
Accepted 10 NOV 2015
Accepted article online 13 NOV 2015
Published online 2 DEC 2015

Vegetation regulation on streamflow intra-annual variability through adaption to climate variations

Sheng Ye[1,2], Hong-Yi Li[2], Shuai Li[3], L. Ruby Leung[2], Yonas Demissie[4], Qihua Ran[1], and Günter Blöschl[5]

[1]Institute of Hydrology and Water Resources, School of Civil Engineering, Zhejiang University, Hangzhou, China, [2]Pacific Northwest National Laboratory, Richland, Washington, USA, [3]Three Gorges Construction and Operation Management Department, China Three Gorges Corporation, Yichang, China, [4]Department of Civil and Environmental Engineering, Washington State University, Pullman, Washington, USA, [5]Institute for Hydraulic and Water Resources Engineering, Vienna University of Technology, Vienna, Austria

Abstract This study aims to provide a mechanistic explanation of the empirical patterns of streamflow intra-annual variability revealed by watershed-scale hydrological data across the contiguous United States. A mathematical extension of the Budyko formula with explicit account for the soil moisture storage change is used to show that, in catchments with a strong seasonal coupling between precipitation and potential evaporation, climate aridity has a dominant control on intra-annual streamflow variability. But in other catchments, additional factors related to soil water storage change also have important controls on how precipitation seasonality propagates to streamflow. More importantly, use of leaf area index as a direct and indirect indicator of the above ground biomass and plant root system, respectively, reveals the vital role of vegetation in regulating soil moisture storage and hence streamflow intra-annual variability under different climate conditions.

1. Introduction

Water and energy are essential elements of catchment hydrology. They are closely linked through evapotranspiration, that is, regulated strongly by plants [*Sivapalan et al.*, 2011]. Despite the complicated interactions among climate, topography, soil, and vegetation [*Ponce and Shetty*, 1995; *Leung et al.*, 2011; *Troch et al.*, 2013; *Li et al.*, 2014], the partitioning of precipitation between evaporation and streamflow is governed to first order by the competition between water supply (precipitation, P) and energy availability (potential evaporation, EP) [*Budyko*, 1974]. The ratio of mean annual potential evaporation and mean annual precipitation (EP/P) is defined as aridity index (ϕ). Characteristic of the long-term climate, ϕ evaporation to precipitation or aridity index has been used to explain different aspects of the landscape hydrological cycles such as streamflow variability [*Koster and Suarez*, 1999], drainage density [*Wang and Wu*, 2013], flow recession [*Ye et al.*, 2014], flood frequency [*Guo et al.*, 2014], event runoff coefficients [*Merz and Blöschl*, 2009], and runoff predictions in ungaged basins [*Parajka et al.*, 2013; *Salinas et al.*, 2013].

Aridity index, however, does not fully explain all the variability in landscape hydrology. Through extensive analyses of the aridity index worldwide, it has been demonstrated that the Budyko prediction of the partitioning between evaporation and streamflow based on aridity index is more skillful in humid catchments where precipitation and potential evaporation are in phase and snowmelt has limited impact [*Sankarasubramanian et al.*, 2001]. When the seasonality of precipitation is significant and/or out of phase with the seasonality of energy, the Budyko hypothesis tends to underestimate runoff [*Milly*, 1994; *Zhang et al.*, 2001; *Potter et al.*, 2005; *Pangle et al.*, 2014]. Due to the steady state assumption at mean annual scale, the Budyko hypothesis falls short at seasonal scale when nonstationary processes such as soil moisture storage must be considered [*Greve et al.*, 2015].

Building on the Budyko hypothesis, many studies have investigated the generation of runoff from precipitation at annual time scale and the seasonality impact on hydrologic cycle. Only a few studies have investigated how catchments filter the intra-annual variability of climate. *Zeng and Cai* [2015] studied the combined impact of climate and catchment storage on evapotranspiration variance. Climate seasonality can propagate to streamflow through soil water storage [*Sankarasubramanian and Vogel*, 2003; *Hickel and Zhang*, 2006; *Gerrits et al.*, 2009; *Parajka et al.*, 2009; *Feng et al.*, 2012]. The interaction between climate and vegetation and with other variables adds additional complexity [*Gentine et al.*, 2012; *McGrath et al.*, 2011; *Pelletier et al.*, 2013; *Perdigão and Blöschl*, 2014]. *Troch et al.* [2009]

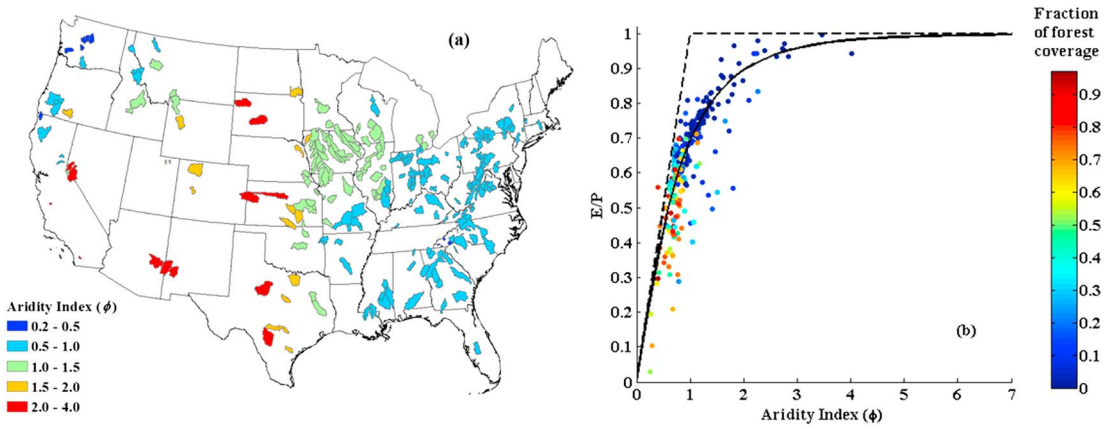

Figure 1. (a) Map of the selected 259 study catchments and (b) Budyko plot of the 259 catchments; the colors indicate the fraction of forest coverage.

hypothesized that vegetation develops to maximize soil moisture use and minimize water stress [also see *Rodriguez-Itube et al.*, 1999]. To achieve this optimality, shallow roots are common in humid catchments with sufficient water supply [*Laio et al.*, 2006], but vegetation in semiarid catchments develops a rooting system that extends more vertically and laterally to tap available moisture [*Gentine et al.*, 2012], similar to the adaption strategy used by vegetation in catchments where precipitation and energy are out of phase [*Gerrits et al.*, 2009]. However, the effect of vegetation seasonality on intra-annual streamflow variability is not fully understood.

This study explores the propagation of intra-annual variability from climate to streamflow and examines the role of vegetation in this process. Using observations from catchments across the U.S. (section 2), patterns obtained from empirical data analysis are interpreted based on an analytical derivation of the Budyko curve by *Koster and Suarez* [1999] but extended to intra-annual time scale (section 3). This allows for an examination of the controlling factors and the role of vegetation properties on the propagation from precipitation to streamflow (sections 4 and 5). The results are summarized and discussed in section 6.

2. Data

Data for 259 catchments across the continental United States spanning a range of climate conditions and physiographic areas are used in this study (Figure 1). These catchments are chosen for their 50 years of continuous daily records of climate and streamflow from 1951 to 2000. The daily precipitation, runoff, and maximum and minimum temperature data are part of the Model Parameter Estimation Experiment (MOPEX) data set [*Duan et al.*, 2005]. Daily potential evaporation (EP) is calculated based on daily maximum, minimum, and mean temperature using the Hargreaves method [*Hargreaves and Samani*, 1985] to represent interannual variability. The estimated EP is scaled to match the mean annual EP provided by MOPEX to ensure consistency with the rainfall and runoff observations. Although the temperature-based estimation of EP could be biased in changing climate or when the surface energy flux components vary drastically [*Sheffield et al.*, 2012], we believe this method to be suitable here since our focus is on the within year variability of the mean monthly water balance components where long term variations are less important. After aggregating the daily climate and streamflow data into monthly records, the abcd-snow model [*Martinez and Gupta*, 2010] is applied to the 259 catchments to estimate the actual evaporation (E). The soil water storage change is then derived as $\Delta S = P - Q - E$.

The vegetation data used in this study include land use type coverage and representative leaf area index (LAI) for each vegetation type. The percentage of each vegetation type is provided by the MOPEX data set based on the University of Maryland vegetation classification with 14 classes in total. As the climate aridity increases across the continental U.S., the fraction of forest coverage decreases and E/P increases (Figure 1b). The characteristic LAI monthly profiles for each vegetation type from the static land cover map provided by NASA's North America Land Data Assimilation System based on satellite images (http://ldas.gsfc.nasa.gov/nldas/NLDASmapveg.php) are used to develop the composite LAI profile for each catchment as the weighted average of the representative LAI of each vegetation type present within the catchment.

To quantify the seasonal variation, several statistical metrics including variance, covariance, and the coefficient of variation of the data are calculated. Monthly climate and hydrologic data obtained from online data set are aggregated from daily observations. The intra-annual standard deviation is calculated from the averaged monthly values over the 50 years for precipitation (σ_P), runoff (σ_Q), potential evaporation (σ_{EP}), and storage change ($\sigma_{\Delta S}$). The intra-annual standard deviation ratio (SDR) between runoff and precipitation is defined as σ_Q/σ_P, similar to the interannual standard deviation ratio defined by *Koster and Suarez* [1999]. Covariance of potential evaporation and precipitation ($\sigma_{EP,P}$), precipitation and storage change ($\sigma_{P,\Delta S}$), and potential evaporation and storage change ($\sigma_{EP,\Delta S}$) are also derived in the same way. The coefficient of variation is also calculated for the LAI to represent the seasonality of vegetation growth: $CV(LAI) = \sigma_{LAI}/\mu_{LAI}$, where σ_{LAI} is the standard deviation of the mean monthly LAI and μ_{LAI} is the annual mean of the monthly representative LAI.

3. Analytical Derivation for Intra-annual SDR Between Runoff and Precipitation

As Budyko proposed in 1974, the behavior of the mean annual evaporation (E) is mainly dominated by that of the mean annual precipitation (P) and potential evaporation (EP). The ratio between evaporation and precipitation (E/P) varies as a function of ϕ:

$$\frac{E}{P} = f(\phi) = \left[\phi\left(\tanh\frac{1}{\phi}\right)(1 - \cosh\phi + \sinh\phi)\right]^{1/2} \tag{1}$$

Figure 1b demonstrates the validity of this relationship, known as the Budyko curve (black line), for the 259 catchments across the continental U.S. Only a few catchments in the Midwest with noticeable anthropogenic influence deviate slightly from the curve [*Wang and Hejazi*, 2011]. As those catchments still follow the Budyko curve to first order, they are included in our analysis to represent a more diverse set of vegetation types.

Assuming that the interannual storage change can be ignored to first order, *Koster and Suarez* [1999] rewrote equation (1) for a given year i as:

$$\frac{E_i}{P_i} = f(\phi_i). \tag{2}$$

Given our focus on intra-annual variance, however, the terrestrial water storage change is no longer negligible, which, at short time scale, supplies moisture for evapotranspiration apart from the direct rainfall [*Greve et al.*, 2015]; hence, equation (2) can be rewritten as

$$\frac{E_j}{P_j - \Delta S_j} = f\left(\frac{EP_j}{P_j - \Delta S_j}\right). \tag{3}$$

Following *Koster and Suarez* [1999], equation (3) is rearranged and linearized about P, ΔS, and ϕ, assuming that the long term mean storage change is close to 0, so that the long term mean of $\frac{EP_j}{P_j - \Delta S_j}$ can be considered equal to ϕ, we obtain

$$\delta E_j = [f(\phi) - \phi f'(\phi)]\delta P_j - [f(\phi) - \phi f'(\phi)]\delta\Delta S_j + f'(\phi)\delta EP_j, \tag{4}$$

where δ denotes the deviation of the value at month j from its long term mean value. Since the long-term mean water storage change is assumed equal to 0, the deviation of soil water storage change at month j from the long term mean ($\delta\Delta S_j$) is indeed equivalent to the soil water storage change at month j (ΔS_j); so for simplicity, we will use ΔS_j in the following equations. This equation is consistent with equation (12) in *Zeng and Cai* [2015].

Since our goal is to understand the impact of catchment filtering from precipitation to streamflow, to better compare with the observed discharge data, we convert δE_j to δQ_j by:

$$\delta Q_j = [1 - f(\phi) + \phi f'(\phi)]\delta P_j - [1 - f(\phi) + \phi f'(\phi)]\Delta S_j - f'(\phi)\delta EP_j. \tag{5}$$

Taking the square of δQ_j and summing over the year, we obtain

$$\begin{aligned}\sigma_Q^2 = {} & [1 - f(\phi) + \phi f'(\phi)]^2\sigma_P^2 + [1 - f(\phi)]^2\sigma_{\Delta S}^2 + f'(\phi)^2\sigma_{EP}^2 - 2[1 - f(\phi)][1 - f(\phi) + \phi f'(\phi)]\sigma_{P,\Delta S} \\ & + 2[1 - f(\phi)]f'(\phi)\sigma_{EP,\Delta S} - 2f'(\phi)[1 - f(\phi) + \phi f'(\phi)]\sigma_{EP,P}\,,\end{aligned} \tag{6}$$

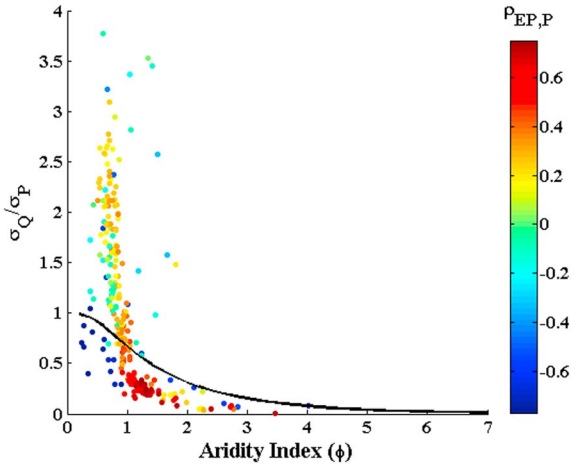

Figure 2. Scatterplot of the observed intra-annual standard deviation ratio between runoff and precipitation versus the aridity index (ϕ). Colors indicate the coefficient of correlation between EP and P ($\rho_{EP,P} = \sigma_{EP,P}/[\sigma_{EP} \times \sigma_P]$). The solid line represents equation (8), a function defined by aridity index only.

where σ_Q^2, σ_P^2, and σ_{EP}^2 are the variance of streamflow, precipitation, and potential evaporation, respectively, while $\sigma_{P,\Delta S}$, $\sigma_{EP,\Delta S}$, and $\sigma_{EP,P}$ refer to the covariance of precipitation and storage change, covariance of potential evaporation and storage change, and covariance of precipitation and potential evaporation at a monthly time scale. Dividing equation (6) by σ_P^2 and taking the square root on both sides, we obtain the standard deviation ratio (SDR) between runoff and precipitation as follows:

$$\frac{\sigma_Q}{\sigma_P} = \{[1-f(\phi)+\phi f'(\phi)]^2 + [1-f(\phi)]^2 \frac{\sigma_{\Delta S}^2}{\sigma_P^2} + f'(\phi)^2 \frac{\sigma_{EP}^2}{\sigma_P^2} - 2[1-f(\phi)][1-f(\phi)+\phi f'(\phi)] \frac{\sigma_{P,\Delta S}}{\sigma_P^2} + 2[1-f(\phi)]f'(\phi)\frac{\sigma_{EP,\Delta S}}{\sigma_P^2} - 2f'(\phi)[1-f(\phi)+\phi f'(\phi)]\frac{\sigma_{EP,P}}{\sigma_P^2}\}1/2. \quad (7)$$

At interannual scale, *Koster and Suarez* [1999] simplified this SDR to a unique function of ϕ:

$$\frac{\sigma_Q}{\sigma_P} = 1 - f(\phi) + \phi f'(\phi). \quad (8)$$

However, at intra-annual scale, none of the quantities in equation (7) can be ignored, so ϕ is not the single dominant factor in the variance propagation from precipitation to streamflow at intra-annual scale. Thus, despite the complexity, equation (7) is used including all the terms in our analysis. See Figure S1 in the supporting information for validation of the derivation using observation data.

4. Controlling Factors of Intra-annual SDR Between Runoff and Precipitation

As shown in Figure 2, the intra-annual SDR of runoff and precipitation decreases with ϕ. The SDR decreases rapidly with increasing ϕ for humid catchments, but for semiarid and arid catchments with $\phi > 1$, the SDR falls within a narrow range between 0 and 0.5. The solid line in Figure 2 is calculated from equation (8), where ϕ is the only variable. Clearly, this simple function of ϕ cannot explain the observed pattern; unlike the interannual SDR values, the intra-annual ones are not necessarily smaller than one. That is, the seasonal variability of runoff can be larger than that of precipitation. For example, in the Appalachian Mountain catchments, rainfall exhibits small seasonality, but runoff has an obvious peak in spring and a minimum in late summer [*Ye et al.*, 2012].

One factor that may influence the propagation of intra-annual variability from precipitation to streamflow is the coupling of precipitation and potential evaporation. As can be seen from Figure 2, the catchments can be divided into two groups. One group consists of catchments with SDR values below or close to equation (8) (solid line) and another group of catchments with SDR values significantly above equation (8). Catchments in the former group are colored dark red and dark blue, indicating a strong positive or negative correlation between P and EP, while catchments of the latter group mostly have smaller coefficient of correlation ($-0.3 < \rho < 0.3$). This suggests that in catchments with strong positive/negative correlation between P and EP, the propagation of variability from climate to streamflow generally follows the trend of the solid line which is monotonically controlled by ϕ following equation (8). That is, for these catchments, the hydrologic processes filtering the variability are closely related to the long-term climate condition, as indicated by ϕ.

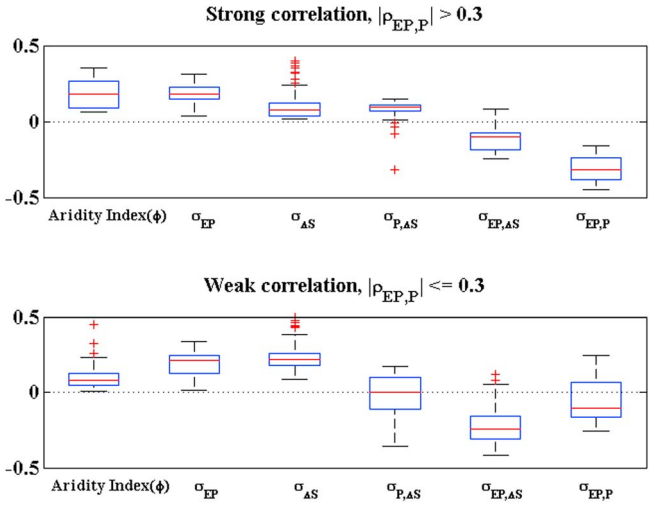

Figure 3. Box plot of the fractional contribution of each component (with coefficient included) in equation (7) for the catchments with (top) strong correlation between EP and P ($\rho > 0.3$ or $\rho < -0.3$) and (bottom) weak correlation ($-0.3 <= \rho <= 0.3$).

For the catchments where water and energy supply (precipitation and potential evaporation) are loosely coupled, other components in equation (7), i.e., soil water storage and its interaction with the climate, control how intra-annual variability of precipitation propagates to that of streamflow.

Breaking down the intra-annual SDR as shown in equation (7), we can calculate the contribution of each term on the right hand side of equation (7) to the SDR. As we can see from Figure 3, in catchments with strong correlation between P and EP, climate conditions (ϕ, σ_{EP}, and $\sigma_{EP,P}$) contribute the most to the SDR, with $\sigma_{EP,P}$ having the largest effect due to the classification criterion, while the storage change and its interaction with climate exert limited control on the SDR value. Thus, compared to the other group, this group of catchments follows the solid line defined by the aridity index alone more closely as shown in Figure 2; the small values of SDR are a result of the net balance among the three larger climate-related terms. On the other hand, for catchments with weak correlation between P and EP, the contribution of soil water storage change and its covariance with climate become more dominant, while the contribution of $\sigma_{EP,P}$ decreases. Consistent with Figure 2, neither the ϕ nor $\sigma_{EP,P}$ can explain the large variations of SDR in these catchments, as other terms in equation (7) have similar magnitudes. The importance of soil water storage change identified here is consistent with the seasonal water storage change effect on the annual water balance [*Sankarasubramanian and Vogel*, 2003; *Hickel and Zhang*, 2006; *Gerrits et al.*, 2009; *Feng et al.*, 2012].

5. Interactions Between Vegetation, Climate, and Landscape

Our analyses have identified an important role of soil water storage change in the intra-annual SDR of runoff to precipitation in catchments with weak coupling between EP and P (e.g., the Appalachian mountainous catchments, the arid catchments in the south, etc.). To better understand the variance of soil water storage change and the interaction between soil storage change with climate (i.e., EP and P), we explore the role of vegetation, as it exerts significant control on evapotranspiration that influences soil water storage. Despite the human impacted catchments in the Midwest that are included for vegetation diversity, the MOPEX catchments are useful for exploring the interactions of vegetation with catchment hydrology in relatively natural conditions. Figure 4 shows the scatterplots between each factor in equation (7) and coefficient of variation (CV)(LAI), which represents seasonal vegetation growth. Except for the larger scatter between ϕ and σ_{EP} with CV(LAI) (Figures 4a and 4b), $\sigma_{\Delta S}$, $\sigma_{P,\Delta S}$, $\sigma_{EP,\Delta S}$, and $\sigma_{EP,P}$ are all closely related to the seasonal growth of vegetation, as shown in Figures 4c–4f, respectively.

More specifically, $\sigma_{\Delta S}$ decreases with the variability of vegetation growth (Figure 4c), suggesting that for catchments with hardy vegetation type (i.e., evergreen forest), soil water storage variation is significant. Conversely, in catchments with larger seasonal vegetation growth, the variation in soil water storage change is relatively smaller, which may be related to the smaller water uptake by these seasonal vegetation (i.e., deciduous forest, prairies, etc.) and the synchronism between EP and P in these catchments.

Similar to $\sigma_{\Delta S}$, the $\sigma_{P,\Delta S}$ also decreases with CV(LAI) (Figure 4d), but $\sigma_{EP,\Delta S}$ increases with the variability of vegetation growth (Figure 4). The less seasonal the vegetation cover, the more synchronous is the soil water storage change with climate (i.e., positive covariance with P and negative covariance with EP). In other words, from evergreen catchments (mostly in the western and southeastern U.S.) to deciduous forests or grassland

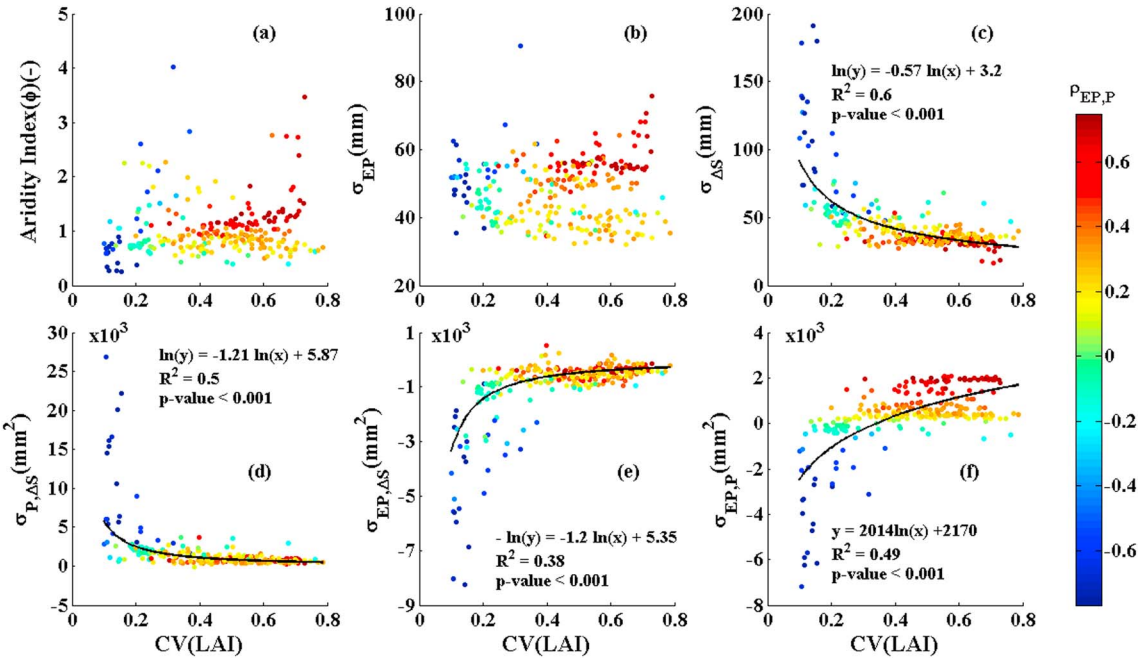

Figure 4. Scatterplots between the coefficient of variation of LAI and each component in equation (7): (a) aridity index, (b) standard deviation of EP, (c) standard deviation of water storage change, (d) covariance of *P* and water storage change, (e) covariance of EP and water storage change, and (f) covariance of EP and *P*; colors indicate the correlation between EP and *P*. Each point represents one catchment and all variances here are temporal ones based on multiyear averaged monthly time steps.

(mostly in the northeast, southern, and central U.S.), the soil water storage change is less correlated with the climate (EP and *P*). This may be related to the low soil water storage capacity of recurrent vegetation and its low water demand in the nongrowing season.

$\sigma_{EP,P}$, an indicator of climate seasonality, has a positive relationship with the vegetation growth variability (Figure 4f). Negative values in $\sigma_{EP,P}$ indicate that rainfall and potential evaporation (energy availability) are out of phase. In catchments with Mediterranean climate, such as those in the Pacific Northwest region, soil water storage can be significant because water availability and evaporative demand are out of phase. The soil water storage can support persistent vegetation growth of evergreen forests during the growing season even when precipitation is limited as long as there is an extended root system that elevates the soil water storage capacity [*Schenk and Jackson*, 2002a, 2002b]. Alternatively catchments with out-of-phase climate seasonality and low CV(LAI) could be covered by desert vegetation with very low LAI year round, but this combination of vegetation and climate is rarely seen in the continental U.S. except perhaps in the southwestern U.S. As the water cycle and energy cycle are more synchronous, evaporation can be large, so soil water storage is low. The relatively drier catchments of this type can only support seasonal vegetation growth, so leaf area peaks in summer and drops in winter. Combined with Figure 4c showing the water storage change variability against the variability of LAI, we can hypothesize that vegetation maintains its growth by maximizing the use of available soil moisture afforded by the out-of-phase relationship between *P* and EP through an extensive root system. In catchments where the water cycle and energy cycle are in phase, vegetation receives the maximum amount of precipitation during its growing season when the evapotranspiration is maximized. With such synchronous water demand and supply cycles, there is no need for a large soil water storage capacity to maintain a moisture surplus to meet the out-of-phase evaporative demand. Rather than stretching the roots vertically and horizontally to increase the moisture supply to cope with the variability in water and energy competition, vegetation varies the primary production seasonally to adapt to the seasonality in climate. This is consistent with previous findings [*Potter et al.*, 2005; *Gentine et al.*, 2012] that plants tend to develop more sophisticated root systems in Mediterranean climates to buffer the discrepancy between precipitation and radiation.

The regression lines in Figures 4c–4f indicate strong correlation between vegetation growth variability and the variance and covariance between precipitation, soil water storage change, and potential evaporation. The natural logarithms of $\sigma_{\Delta S}$, $\sigma_{P,\Delta S}$, and $\sigma_{EP,\Delta S}$ all vary linearly with CV(LAI), with p-values less than 0.001, indicating statistically significant relationships. For $\sigma_{EP,P}$ (Figure 4f), the relationship is fitted with a logarithmic function rather than applying a linear regression to the log values since the covariance spreads across negative and positive values. For three of the four variables, the regressed functions explain more than half of the variance.

Besides the various strong correlations noted above, the asymptotic behaviors in the relationships revealed in Figure 4 deserve further attention. Most catchments have relatively small absolute covariances ($\sigma_{P,\Delta S}$, $\sigma_{EP,\Delta S}$, and $\sigma_{EP,P}$), but a few clearly stands out with large values. By labeling each catchment using color denoting the values of the coefficient of correlation between EP and P, it becomes clear that the outliers in each plot correspond to catchments with large negative $\sigma_{EP,P}$, where precipitation and radiation are out of phase. The importance of the coupling between water and energy cycles has been recognized before [*Gerrits et al*., 2009; *Troch et al*., 2013; *Coopersmith et al*., 2012]. An out-of-phase seasonal relationship between precipitation and radiation leads to a large variance in soil water storage change, as soil water is depleted by evapotranspiration in the summer and refilled in the winter by precipitation. This also explains why the soil water storage change correlates positively and negatively with precipitation and radiation, respectively.

6. Discussion and Conclusion

Following the analytical derivation proposed by *Koster and Suarez* [1999], this study aims to delineate factors that control the propagation of seasonality from climate to streamflow through the catchment hydrologic processes. Using an analytical expression and observation data from MOPEX catchments, we found that the aridity index (ϕ), variance of precipitation (σ_P), potential evaporation (σ_{EP}), storage change ($\sigma_{\Delta S}$), the covariance of precipitation and potential evaporation ($\sigma_{EP,P}$), precipitation and storage change ($\sigma_{P,\Delta S}$), and potential evaporation and storage change ($\sigma_{EP,\Delta S}$) all cast their impacts on the intra-annual SDR between rainfall and runoff. Statistical analyses indicate that besides ϕ, whose importance has been recognized before, coupling of the seasonality in precipitation and potential evaporation is also a critical factor on catchments' hydrologic responses to the intra-annual variability in climate. The role of other factors such as $\sigma_{\Delta S}$ and $\sigma_{P,\Delta S}$ is dependent on whether the water and energy cycles are out of phase or synchronous.

Correlating the influential factors with the vegetation growth variation in Figure 4 reveals a vital role of vegetation in regulating soil moisture through evapotranspiration. The positive logarithmic relationship between $\sigma_{EP,P}$ and CV(LAI), along with the negative correlation between CV(LAI) and $\sigma_{\Delta S}$, shed lights on the vegetation water use strategy under different climates.

In general, our results suggest that vegetation has two major approaches to adapt to the variability in water supply and demand: by extending the root profiles to access more water to support the above ground biomass or by varying the primary production seasonally when the soil moisture capacity is limited for storage change. For example, in humid Mediterranean catchments where the water and energy cycles are out of phase, more persistent vegetation types (i.e., evergreen forests) are established with advanced root system to maximize the use of available soil moisture for above ground biomass production year round. On the other hand, in less humid catchments where EP and P are more synchronous and soil moisture is available mainly in the summer rainy season, plants (e.g., deciduous forests and grasslands) cope with the limited soil water storage by varying the biomass above ground seasonally with the water and energy cycles. This strategy is in line with the analysis of *Schenk and Jackson* [2002a, 2002b] of global root depth, *Gao et al*. [2014] of model simulations on the root zone moisture storage capacity and the findings of *Potter et al*. [2005], and *Gentine et al*. [2012] on the interaction between vegetation above- and below- ground structure and surface hydrology.

To conclude, by examining the climate, hydrology and vegetation data from MOPEX catchments across the continental U.S. using the framework of Budyko's water balance equation, we explored the controlling factors on the propagation of intra-annual variability from climate to streamflow. Besides the well-recognized ϕ, $\sigma_{EP,P}$, and $\sigma_{\Delta S}$ also play important roles. Moreover, climate and soil storage change are interrelated through vegetation dynamics that optimizes water use and biomass production. However, the dominant vegetation in the MOPEX catchments transitions from evergreen forest to grassland and then cropland gradually as the climate

gets drier; the lack of vegetation diversity in the same climate may limit our understanding. It is important to validate our findings in other regions with a wider range of climates for the same vegetation type. Analytical derivations and numerical experiments are also needed to further explain the patterns we found between the variance in climate, vegetation growth, soil water storage change, and the resulting hydrologic responses.

Acknowledgments
This research was supported by the Office of Science of the U.S. Department of Energy as part of the Regional and Global Climate Modeling Program and Earth System Modeling Program. The Pacific Northwest National Laboratory is operated for DOE by Battelle Memorial institute under contract DE-AC05-76RLO 1830. The last author would like to thank the Austrian Academy of Sciences (project on Predictability of runoff in a changing environment) for financial support.

References

Budyko, M. I. (1974), *Climate and Life*, Elsevier, New York.
Coopersmith, E., M. A. Yaeger, S. Ye, L. Chengand, and M. Sivapalan (2012), Exploring the physical controls of regional patterns of flow duration curves—Part 3: A catchment classification system based on regime curve indicators, *Hydrol. Earth Syst. Sci.*, *16*, 4467–4482, doi:10.5194/hess-16-4467-2012.
Duan, Q., J. Schaake, V. Andreassian, S. Franks, H. Gupta, Y. Gusev, F. Habets, A. Hall, L. Hay, and T. Hogue (2005), Model parameter estimation experiment (MOPEX): Overview and summary of the second and third workshop results, *J. Hydrol.*, *320*, 3–17.
Feng, X., G. Vico, and A. Porporato (2012), On the effects of seasonality on soil water balance and plant growth, *Water Resour. Res.*, *48*, W05543, doi:10.1029/2011WR011263.
Gao, H., M. Hrachowitz, S. J. Schymanski, F. Fenicia, N. Sriwongsitanon, and H. H. G. Savenije (2014), Climate controls how ecosystems size the root zone storage capacity at catchment scale, *Geophys. Res. Lett.*, *41*, 7916–7923, doi:10.1002/2014GL061668.
Gentine, P., P. D'Odorico, B. R. Lintner, G. Sivandran, and G. Salvucci (2012), Interdependence of climate, soil, and vegetation as constrained by the Budyko curve, *Geophys. Res. Lett.*, *39*, L19404, doi:10.1029/2012GL053492.
Gerrits, A. M. J., H. H. G. Savenije, E. J. M. Veling, and L. Pfister (2009), Analytical derivation of the Budyko curve based on rainfall characteristics and a simple evaporation model, *Water Resour. Res.*, *45*, W04403, doi:10.1029/2008WR007308.
Greve, P., L. Gudmundsson, B. Orlowsky, and S. I. Seneviratne (2015), The Budyko framework beyond stationarity, *Hydrol. Earth Syst. Sci. Discuss.*, *12*, 6799–6830.
Guo, J., H.-Y. Li, L. R. Leung, S. Guo, P. Liu, and M. Sivapalan (2014), Links between flood frequency and annual water balance behaviors: A basis for similarity and regionalization, *Water Resour. Res.*, *50*, 937–953, doi:10.1002/2013WR014374.
Hargreaves, G. H., and Z. A. Samani (1985), Reference crop evapotranspiration from temperature, *Appl. Eng. Agric.*, *1*(2), 96–99.
Hickel, K., and L. Zhang (2006), Estimating the impact of rainfall seasonality on mean annual water balance using a top-down approach, *J. Hydrol.*, *331*, 409–424.
Koster, R. D., and M. J. Suarez (1999), A simple framework for examining the interannual variability of land surface moisture fluxes, *J. Clim.*, *12*, 1911–1917.
Laio, F., P. D'Odorico, and L. Ridolfi (2006), An analytical model to relate vertical root distribution to climate and soil properties, *Geophys. Res. Lett.*, *33*, L18401, doi:10.1029/2006GL027331.
Leung, L. R., M. Huang, Y. Qian, and X. Liang (2011), Climate-soil-vegetation control on groundwater table dynamics and its feedbacks in a climate model, *Clim. Dyn.*, *36*(1–2), 57–81, doi:10.1007/s00382-010-0746-x.
Li, H., M. Sivapalan, F. Tian, and C. Harman (2014), Functional approach to exploring climatic and landscape controls of runoff generation. 1. Behavioral constraints on runoff volume, *Water Resour. Res.*, *50*, 9300–9322, doi:10.1002/2014WR016307.
Martinez, G. F., and H. V. Gupta (2010), Toward improved identification of hydrological models: A diagnostic evaluation of the "abcd" monthly water balance model for the conterminous United States, *Water Resour. Res.*, *46*, W08507, doi:10.1029/2009WR008294.
McGrath, G. S., K. Paik, and C. Hinz (2011), Complex landscapes from simple ecohydrological feedbacks, in *MODSIM2011, 19th International Congress on Modelling and Simulation*, edited by F. Chan, D. Marinova, and R. S. Anderssen, pp. 2528–2534, Model. and Simul. Soc. of Australia and New Zealand, Canberra.
Merz, R., and G. Blöschl (2009), A regional analysis of event runoff coefficients with respect to climate and catchment characteristics in Austria, *Water Resour. Res.*, *45*, W01405, doi:10.1029/2008WR007163.
Milly, P. C. D. (1994), Climate, interseasonal storage of soil-water, and the annual water balance, *Adv. Water Resour.*, *17*(1–2), 19–24, doi:10.1016/0309-1708(94)90020-5.
Pangle, L. A., J. W. Gregg, and J. J. McDonnell (2014), Rainfall seasonality and an ecohydrological feedback offset the potential impact of climate warming on evapotranspiration and groundwater recharge, *Water Resour. Res.*, *50*, 1308–1321, doi:10.1002/2012WR013253.
Parajka, J., S. Kohnová, R. Merz, J. Szolgay, K. Hlavcová, and G. Blöschl (2009), Comparative analysis of the seasonality of hydrological characteristics in Slovakia and Austria, *Hydrol. Sci. J.*, *54*(3), 456–473.
Parajka, J., A. Viglione, M. Rogger, J. L. Salinas, M. Sivapalan, and G. Blöschl (2013), Comparative assessment of predictions in ungauged basins—Part 1: Runoff hydrograph studies, *Hydrol. Earth Syst. Sci.*, *17*, 1783–1795.
Pelletier, J. D., et al. (2013), Coevolution of nonlinear trends in vegetation, soils, and topography with elevation and slope aspect: A case study in the sky islands of southern Arizona, *J. Geophys. Res. Earth Surf.*, *118*, 741–758, doi:10.1002/jgrf.20046.
Perdigão, R. A. P., and G. Blöschl (2014), Spatiotemporal flood sensitivity to annual precipitation: Evidence for landscape-climate coevolution, *Water Resour. Res.*, *50*, 5492–5509, doi:10.1002/2014WR015365.
Ponce, V. M., and A. V. Shetty (1995), A conceptual model of catchment water balance. 1. Formulation and calibration, *J. Hydrol.*, *173*, 27–40.
Potter, N. J., L. Zhang, P. C. D. Milly, T. A. McMahon, and A. J. Jakeman (2005), Effects of rainfall seasonality and soil moisture capacity on mean annual water balance for Australian catchments, *Water Resour. Res.*, *41*, W06007, doi:10.1029/2004WR003697.
Rodriguez-Itube, I., P. D'Odorico, A. Porporato, and L. Ridolfi (1999), Tree-grass coexistence in savannas: The role of spatial dynamics and climate fluctuations, *Geophys. Res. Lett.*, *26*(2), 247–250.
Salinas, J. L., G. Laaha, M. Rogger, J. Parajka, A. Viglione, M. Sivapalan, and G. Blöschl (2013), Comparative assessment of predictions in ungauged basins—Part 2: Flood and low flow studies, *Hydrol. Earth Syst. Sci.*, *17*, 2637–2652, doi:10.5194/hess-17-2637-2013.
Sankarasubramanian, A., and R. M. Vogel (2003), Hydroclimatology of the continental United States, *Geophys. Res. Lett.*, *30*(7), 1363, doi:10.1029/2002GL015937.
Sankarasubramanian, A., R. M. Vogel, and J. F. Limbrunner (2001), Climate elasticity of streamflow in the United States, *Water Resources Res.*, *37*(6), 1771–1781, doi:10.1029/2000WR900330.
Schenk, H. J., and R. B. Jackson (2002a), Rooting depths, lateral root spreads and below-ground/above-ground allometries of plants in water-limited ecosystems, *J. Ecol.*, *90*(3), 480–494.
Schenk, H. J., and R. B. Jackson (2002b), The global biogeography of roots, *Ecol. Monogr.*, *72*(3), 311–328.

Sheffield, J., E. F. Wood, and M. L. Roderick (2012), Little change in global drought over the past 60 years, *Nature*, *491*(7424), 435–438, doi:10.1038/nature11575.

Sivapalan, M., M. A. Yaeger, C. J. Harman, X. Xu, and P. A. Troch (2011), Functional model of water balance variability at the catchment scale: 1. Evidence of hydrologic similarity and space-time symmetry, *Water Resour. Res.*, *47*, W02522, doi:10.1029/2010WR009568.

Troch, P. A., G. F. Martinez, V. R. N. Pauwels, M. Durcik, M. Sivapalan, C. Harman, P. D. Brooks, H. Gupta, and T. Huxman (2009), Climate and vegetation water use efficiency at catchment scales, *Hydrol. Processes*, *23*(16), 2409–2414, doi:10.1002/hyp.7358.

Troch, P. A., G. Carrillo, M. Sivapalan, T. Wagner, and K. Sawicz (2013), Climate-vegetation-soil interactions and long-term hydrologic partitioning: Signatures of catchment co-evolution, *Hydrol. Earth Syst. Sci.*, *17*, 2209–2217.

Wang, D., and M. Hejazi (2011), Quantifying the relative contribution of the climate and direct human impacts on mean annual streamflow in the contiguous United States, *Water Resour. Res.*, *47*, W00J12, doi:10.1029/2010WR010283.

Wang, D., and L. Wu (2013), Similarity of climate control on base flow and perennial stream density in the Budyko framework, *Hydrol. Earth Syst. Sci.*, *17*, 315–324.

Ye, S., M. Yaeger, E. Coopersmith, L. Cheng, and M. Sivapalan (2012), Exploring the physical controls of regional patterns of flow duration curves—Part 2: Role of seasonality and associated process controls, *Hydrol. Earth Syst. Sci.*, *16*, 4447–4465.

Ye, S., H. Li, M. Huang, M. Ali, L. Leung, S. Wang, and M. Sivapalan (2014), Regionalization of subsurface stormflow parameters of hydrologic models: Derivation from regional analysis of streamflow recession curves, *J. Hydrol.*, *519*, 670–682, doi:10.1016/j.jhydrol.2014.07.017.

Zeng, R., and X. Cai (2015), Assessing the temporal variance of evapotranspiration considering climate and catchment storage factors, *Adv. Water Resour.*, *79*, 51–60.

Zhang, L., W. R. Dawes, and G. R. Walker (2001), Response of mean annual evapotranspiration to vegetation changes at catchment scale, *Water Resour. Res.*, *37*, 701–708.